Theoretical Study on the Identity Ion Pair S_N2 Reactions of LiX with CH_3SX (X = Cl, Br, and I): Structure, Mechanism, and Potential Energy Surface†

Yi Ren,*,‡,§ Jing-Gang Gai,‡ Yan Xiong,‡ Kuo-Hsing Lee,§ and San-Yan Chu*,§

College of Chemistry, Sichuan University, Chengdu, 610064, People's Republic of China, and Department of Chemistry, National Tsing Hua University, Hsinchu 30013, Taiwan

Received: November 13, 2006; In Final Form: February 13, 2007

Three archetypal ion pair nucleophilic substitution reactions at the methylsulfenyl sulfur atom $LiX + CH_3SX \rightarrow XSCH_3 + LiX$ (X = Cl, Br, and I) are investigated by the modified Gaussian-2 theory. Including lithium cation in the anionic models makes the ion pair reactions proceed along an S_N2 mechanism, contrary to the addition−elimination pathway occurring in the corresponding anionic nucleophilic substitution reactions $X^- + CH_3SX \rightarrow XSCH_3 + X^-$. Two reaction pathways for the ion pair S_N2 reactions at sulfur, inversion and retention, are proposed. Results indicate the inversion pathway is favorable for all the halogens. Comparison of the transition structures and energetics for the ion pair S_N2 at sulfur with the potential competition ion pair S_N2 reactions at carbon $LiX + CH_3SX \rightarrow XCH_3 + LiXS$ shows that the S_N2 reactions at carbon are not favorable from the viewpoints of kinetics and thermodynamics.

1. Introduction

In the past decade, nucleophilic substitution reactions at formal neutral sulfur have become the focus of attention because of their synthetic, biochemical, and theoretical importance.[1] Displacement reactions at heteroatoms, featured widely in both organic and bioorganic compounds, are the most important processes in metabolism.[1b] There are indications that the mechanisms are different between first- and second-row atoms. A classic S_N2 mechanism is evident for anionic nucleophilic substitution at carbon [S_N2(C)],[2] at nitrogen [S_N2(N)],[3] and at oxygen [S_N2(O)],[4] but an addition−elimination (A−E) pathway occurs for substitution at silicon[5] and phosphorus.[6] As for substitution at sulfur, there are two mechanisms proposed by different research groups. Experimental studies of nucleophilic substitution at dicoordinated sulfur in benzene by Ciuffarin et al. argued that the relative reaction rates are best interpreted via an A−E mechanism.[7] Ciuffarin also measured the effect of the basicity of the leaving group in the reaction of pyridine and butylamine with para-substituted $Ph_3CSO-C_6H_4X$ and revealed a mechanistic dependence on the nucleophile and the leaving group.[8] Kice et al. examined the nucleophilic substitution at sulfenyl, sulfinyl, and sulfonyl centers, and concluded that substitution at sulfenyl center may proceed with an A−E pathway.[9] However, thiolate and cyanide attack of the sulfenyl center of phenyl benzenethiosulfonate shows evidence of an S_N2 mechanism.[10]

Theoretically, Bachrach et al. made various comprehensive studies on the mechanism of anionic substitution reactions at sulfur.[11] In 1996, they examined three gas-phase thiolate−disulfide exchange reactions (eq 1)[11a] using ab initio method. Their results indicate that the

$$R_1S^- + R_2SSR_3 \rightarrow R_1SSR_2 + R_3S^- \text{(i−iii)} \qquad (1)$$

where (i) $R_1 = R_2 = R_3 = H$; 1(ii) $R_1 = R_3 =$ Me, $R_2 = H$; and (iii) $R_1 = R_3 = H$, $R_2 = Me$

reaction mechanism depends on the theoretical level and size of R_2. At the HF/6-31+G* level, the above three reactions proceed via an S_N2 mechanism. However, a triple-well potential energy surface (PES) is found when a correlation function is used, indicating that the reaction pathway will follow an A−E mechanism (Chart 1a). Structural and energetic results do suggest that as R_2 becomes larger, the reaction may not proceed via an addition−elimination pathway and the S_N2 mechanism (Chart 1b) will operate. They also investigated the nucleophilic substitution reactions involving simple species (Cl^-, PH_2^-, MeO^-, HO^-, NH_2^-) as nucleophiles and leaving groups in methylsulfenyl derivatives ($X^- + CH_3SY \rightarrow YSCH_3 + X^-$) at B3LYP/aug-cc-pVDZ.[11c] The results show that the gas-phase reactions proceed along an A−E pathway as long as the nucleophile is not too strong base. Recently, the reaction of cyclo-L-cystine with thiolate was calculated at the B3LYP/6-31+G* level by Bachrach and his co-workers.[11e] The model system embeds the disulfide bond within a protein-like environment. The computations therefore suggest that gas-phase nucleophilic substitution at sulfur in proteins and gliotoxin will occur by the A−E mechanism. More recently, we performed a theoretical study on the four reactions $X^- + CH_3SCl$ (X = F, Cl, Br, and I) at B3LYP/6-311+G (2df, p) and compared three possible reaction channels, including substitution at sulfur (eq 2), substitution at carbon (eq 3), and deprotonation (eq 4).[12]

$$X^- + CH_3SCl \rightarrow CH_3SX + Cl^- \qquad (2)$$

$$X^- + CH_3SCl \rightarrow XCH_3 + SCl^- \qquad (3)$$

† Part of the special issue "M. C. Lin Festschrift".

* Corresponding authors. Telephone/Fax: 86-28-85257397. E-mail: yiren57@hotmail.com (Y.R.). Telephone: 886-3-5721634. Fax : 886-3-5711082. E-mail: sychu@mx.nthu.edu.tw (S.-Y.C.).

‡ Sichuan University.

§ National Tsing Hua University.

10.1021/jp067495k CCC: $37.00
Published on Web 03/22/2007

$$X^- + CH_3SCl \rightarrow HX + {}^-CH_2SCl \quad (4)$$

Our calculated results indicate that X^- (X = Cl, Br, and I) preferably attacks sulfur instead of the carbon atom of CH_3SCl and the substitution reactions at sulfur follow an A−E mechanism. However, the deprotonation pathway is much more favorable for the reaction of F^- with CH_3SCl because of the stronger basicity of fluoride anion.

However, many important reactions in organic chemistry take place in nonpolar or lower polarity solvents and generally involve neutral *contact*, or *tight* ion pairs as reactants instead of free ions.[13,14] The *contact* ion pair (called ion pair hereinafter) will have significant ionic character, but the ions are not separated by solvent. The reactivity of the ion pair is expected to be rather different from that of the anion species, but theoretical treatments of the ion pair S_N2 reactions are scarce. The systematic studies on the ion pair S_N2 reactions may begin from the work of Streitwieser and co-workers.[15] They calculated some unsolvated identity ion pair S_N2(C) reactions and got some interesting results.[15a] These identity reactions MX + CH_3X (X = F and Cl; M = Li and Na) involve preliminary encounter dipole−dipole complexes and then proceed via a cyclic inversion or retention transition structure (TS) with highly bent X−C−X bonds behaving as assemblies of ions. They also extended the work to the higher alkyls and discussed some steric effects for the ion pair S_N2(C)reactions.[15b] More recently, Ren et al. reported a series of theoretical studies on the ion pair S_N2(C)[16] and S_N2(N)[17] and addressed the influence of Li^+ on the geometries and relative energies of the stationary points on the PESs.

The ion pair bimolecular nucleophilic substitution reactions at sulfur [S_N2(S)] can be widely applied in the synthesis of compounds containing an −S− functional group, e.g., unsymmetrical disulfides (eq 5) and thiosulfonates (eq 6),[18] but no

$$RSNa + R'SX \rightarrow RSSR' + NaX \quad (5)$$

$$RS(=O)ONa + R'SCl \rightarrow RS(=O)OSR' + NaCl \quad (6)$$

theoretical studies were found until now. Before the more realistic systems are studied, it is helpful and useful to investigate the generality of ion pair S_N2(S) reactions using the simple models. In the present study, we report theoretical investigations on the three symmetric and thermoneutral ion pair substitution reactions between lithium halides and methylsulfenyl halides in the gas phase (eqs 7−9).

$$LiCl + CH_3SCl \rightarrow ClSCH_3 + LiCl \quad (7)$$

$$LiBr + CH_3SBr \rightarrow BrSCH_3 + LiBr \quad (8)$$

$$LiI + CH_3SI \rightarrow ISCH_3 + LiI \quad (9)$$

Our objectives here are to explore the possible mechanisms of these archetypal reactions, compare the mechanistic differences between ion pair and anionic substitution reactions, and try to address the origin of S_N2 mechanism with the ion pair as nucleophile. We will also discuss the potential competition reactions with these ion pair substitution reactions at sulfur.

The present work represents the computational study of the fundamental ion pair S_N2(S) reactions at a high level and will hopefully provide reliable energy parameters.

2. Computational Details

Modified Gaussian-2 theory[19] (G2M) was extensively used in the study of the reaction mechanisms.[20] Martin et. al[21] pointed out that the diffusion function is necessary in the structural optimization for the S_N2 reaction. Therefore, when the G2M method was applied to this work, all geometries were fully optimized at the B3LYP level[22] with the 6-311+G(d,p) instead of 6-311G(d,p) basis sets in the original G2M. Vibrational frequencies were employed to characterize stationary points, and the unscaled zero-point energies were included in the comparison of relative energies. Electron correlation effect was evaluated using coupled cluster calculation including triple excitations noniteratively [CCSD(T)]. This level of theory is termed as G2M(+) in the present study. The G2M(+) method has been used in our previous theoretical studies on ion pair S_N2(C)[16a] and S_N2(N)[17] reactions.

All-electron basis sets were used for all first- and second-row atoms, while Hay and Wadt effective core potentials[23] were used for the third- and fourth-row atoms, referred to as G2M-(+)-ECP. Charge distributions were calculated by natural population analysis (NPA)[24] at the MP2/6-311+G(3df,2p) level on B3LYP/6-311+G(d,p) geometries. All calculations were performed with Gaussian 98.[25]

Throughout this paper, all internuclear distances are in angstroms (Å) and bond angles are in degrees (°). Unless other noted, relative energies correspond to enthalpy changes at 0 K [ΔH(0 K)] in kilojoules per mole (kJ/mol).

CHART 1: Schematic Drawings of PESs for the Identity Anionic Nucleophilic Substitution Reactions at Sulfur: A−E Mechanism (a) and S_N2 Mechanism (b)

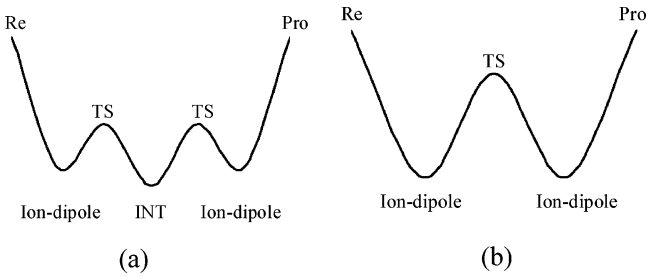

3. Results and Discussion

The energy profile for the ion pair S_N2(S) reactions (eqs 7−9) can be described by a symmetrical double-well-potential curve, which is the characteristic curve for all the classic S_N2 reactions of first-row atoms, including carbon,[2] nitrogen,[3b] and oxygen.[4b] Two possible reaction pathways, corresponding to different mechanisms, inversion and retention, are proposed. The inversion pathway involves the initial formation of a prereaction dipole−dipole complex **1**. This complex must then overcome the central barrier to reach a symmetrical inversion TS **2**. The latter then breaks down to give the product dipole−dipole complex, accompanying the transfer of lithium from incoming halogen to outgoing halogen atom. The product dipole−dipole complex subsequently dissociates into the separate products. For the retention pathway, the complex and TS are denoted as **1′** and **2′**, respectively. The key energetic quantities involved in

$XLi\cdots S(CH_3)X$	$CH_3SX\cdots LiX$	$[X\cdots CH_3SLi\cdots X]^{\neq}$	$[CH_3S\cdots X_2Li]^{\neq}$
1a–c (C_1)	**1′a–c** (C_1)	**2 a–c** (C_s)	**2′a–c** (C_S)

(**a**: X = Cl; **b**: X = Br; **c**: X = I)

reactions (eqs 7−9), as depicted in Scheme 1, are labeled as follows: ΔH_{comp} is the complexation energy for the dipole−dipole complex, here defined as [H(com) − H(LiX) − H(CH_3-SX)]. $\Delta H^{\ddagger}_{cent}$ is the reaction barrier with respect to the complex,

SCHEME 1: Schematic PES for the Identity Ion Pair S_N2(S) Reactions (eqs 7−9)

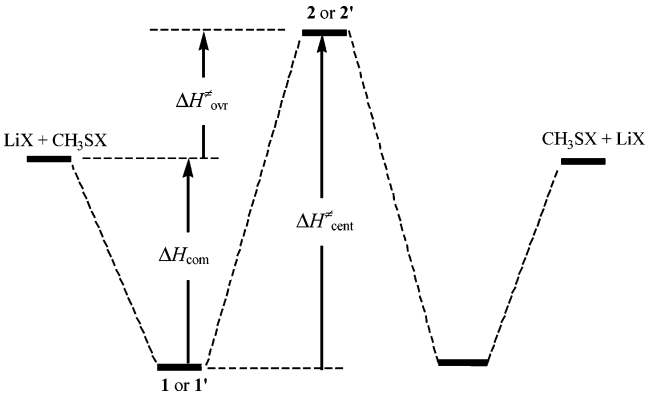

called the central barrier. $\Delta H^{\ddagger}_{ovr}$ is the overall activation barrier relative to the free reactants.

The main geometries of optimized reactants, dipole−dipole complexes, and TSs are shown in Tables 1−3 and Figure 1. All of the energetics involved in eqs 7−9 are listed in Table 4.

3.1. Reactants. Predicted properties of LiX (X = Cl, Br, and I) are compared with experimental and MP2 results in Table 1. The geometries of LiX at the B3LYP/6-311+G(d,p) level agree well with the available experimental[26] and MP2(full)/6-31+G-(d) data.[27] All frequencies and dipole moment values for LiX are reproduced by DFT method. The Li−X bond dissociation energies compare favorably with experimental and G2M(+) values with errors less than about 10 kJ/mol. B3LYP/6-311+G-(d,p) optimized geometric parameters for CH_3SCl also agree reasonably well with the MP2(full)/6-31G(d) values.[28]

3.2. Dipole−Dipole Complexes. Reactions of LiX with CH_3-SX (X = Cl, Br, and I) start with the formation of prereaction complexes. The lithium cation can coordinate with sulfur, forming the inversion complexes XLi···S(CH_3)X (**1a**−**c**), or with halogen, leading to the retention complexes CH_3SX···LiX (**1′a**−**c**). G2M(+) complexation energies, ΔH_{comp}, for **1a**−**c** and **1′a**−**c** vary in a range of just about 3 kJ/mol, much smaller than that (about 20 kJ/mol) for the ion−dipole complexes X^-···CH_3SX. The ΔH_{comp} values decrease in the order X = I (59.2 kJ/mol) > X = Br (57.9 kJ/mol) > X = Cl (56.6 kJ/mol) for **1a**−**c** and X = I (63.9 kJ/mol) > X = Br (61.9 kJ/mol) > X = Cl (61.2 kJ/mol) for **1′a**−**c**, in contrast to the situation in the anionic nucleophilic substitution at sulfur, where the halide ion coordinates with one hydrogen atom in CH_3SCl and the complexation energies for X^-···CH_3SCl (X = Cl, Br, and I) tend to increase in the order $I^- < Br^- < Cl^-$.[12] The complexation of LiX with CH_3SX make the S−X bond distances in the free reactants slightly elongate from 2.093 to 2.115 Å in **1a** or 2.115 Å in **1′a**, from 2.250 to 2.271 Å in **1b** or 2.253 Å in **1′b**, and from 2.438 to 2.458 Å in **1c** or 2.443 Å in **1′c**, which is favorable for the proceeding of the subsequent nucleophilic attack.

3.3. Transition State Structures and Central Barrier Heights. The inversion TSs LiX/CH_3SX (X = Cl, Br, and I) (**2a**−**c**) have C_s symmetry, where lithium coordinates with sulfur and acts as a bridge connecting both halogen atoms. The inversion TSs with inclusion Li cation show smaller deformation from the stable intermediate found in the anionic substitution reactions at sulfur.[12] The bridging actions of Li cation only cause two halogen anions to bend toward it with a decrease of the X−S−X angle by about 35°, which is much smaller than that in the inversion TSs LiX/CH_3X in the ion pair S_N2(C),[16a] where there is a remarkable deformation from the linear TS geometry $[X\cdots CH_3\cdots X]^{-\ddagger}$ found in the anionic S_N2(C) reactions and the Li cation causes a large decrease of the X−C−X angle by about 90°. These may be the main reasons the central barrier heights in the inversion pathway, $\Delta H^{\ddagger}_{cent}$(inv), for the ion pair S_N2(S) are much lower than those in the ion pair S_N2(C) reactions (see Table 4). Calculated G2M(+) $\Delta H^{\ddagger}_{cent}$(inv) values for the ion pair S_N2(S) reactions are significantly lower than those in the corresponding ion pair S_N2(C) reactions by more than 100 kJ/mol (Table 4), decreasing in the order X = Cl (90.6 kJ/mol) > X = Br (69.7 kJ/mol) > X = I (53.3 kJ/mol).

In the retention pathway, the coordination of the lithium cation is on the same side of sulfur to both entering and leaving halide ions (see Figure 1, **2′**), which is similar to the geometries of retention TSs in the ion pair S_N2(C) reactions.[16a] There are more elongations of S−X bond distances (0.337−0.363 Å) and remarkable decreases of X−S−X angles (54.2−76.6°) in the retention LiX/CH_3SX TSs (**2′a**−**c**) relative to the inversion TSs (**2a**−**c**), respectively. These geometric characteristics indicate the retention TSs will be much less stable than the inversion ones.

The retention central barriers, $\Delta H^{\ddagger}_{cent}$(ret), are much higher than the corresponding $\Delta H^{\ddagger}_{cent}$(inv) values, and the energy differences [$\Delta H^{\ddagger}_{cent}$(ret) − $\Delta H^{\ddagger}_{cent}$(inv)] are equal to 87.7, 102.6, and 120.8 kJ/mol for X = Cl, Br, and I, respectively. This probably originates in large part from the stronger electrostatic repulsion between two halide anions and more elongation of the S−X (X = Cl, Br, and I) bonds in the retention TSs (**2′a**−**c**). Accordingly, we will focus on the inversion pathway in the following discussions.

The main geometric features of inversion TSs (**2a**−**c**) are the simultaneous elongations of the Li−X and S−X (X = Cl, Br, and I) bonds relative to the dipole−dipole complexes. We can easily characterize the geometric looseness of Li−X and S−X bonds by parameters %Li−$X^{\ddagger}$ and %S−$X^{\ddagger}$, in a way similar to that proposed for the anionic S_N2 reactions.[2a,3b]

$$\%\text{Li}-\text{X}^{\ddagger} = 100[r^{\ddagger}(\text{Li}-\text{X}) - r^{\text{comp}}(\text{Li}-\text{X})]/r^{\text{comp}}(\text{Li}-\text{X})] \quad (10)$$

$$\%\text{S}-\text{X}^{\ddagger} = 100[r^{\ddagger}(\text{S}-\text{X}) - r^{\text{comp}}(\text{S}-\text{X})]/r^{\text{comp}}(\text{S}-\text{X})] \quad (11)$$

where $r^{\ddagger}$(Li−X), $r^{\ddagger}$(S−X) and r^{comp}(Li−X), r^{comp}(S−X) are the Li−X and S−X bond lengths in the inversion TS **2** and dipole−dipole complex **1**, respectively.

The search for relationships between transition state structures and reaction barriers is an important aspect of physical organic chemistry. Such relationships are of particular interest because of their extensive use by experimentalists. The geometric looseness in the inversion TSs gives an indication of the extent of bond weakening. Computations on the ion pair S_N2 reactions at carbon[16a] and at nitrogen[17b] revealed that the geometric looseness of TS could correlate with the magnitude of the central barrier. Present results show that a larger barrier is associated with a TS having a higher percentage of Li−X and S−X bonds lengthening and the sum of %Li−$X^{\ddagger}$ and %S−$X^{\ddagger}$ correlates well with the magnitude of $\Delta H^{\ddagger}_{cent}$(inv) ($R^2$ = 0.999). This correlation indicates that the stretching of the cleaving Li−X and S−X bonds is the major factor determining the $\Delta H^{\ddagger}_{cent}$-(inv) values. The other factors may be dissociation energies for the Li−X and S−X single bonds (see Tables 1 and 2). This is reasonable because the central barrier heights in the LiX + CH_3-SX (X = Cl, Br, I) reactions should be also governed by these dissociation energies. There is still a good linear relationship (R^2 = 0.999) between $\Delta H^{\ddagger}_{cent}$ and (%Li−$X^{\ddagger}$)D_{Li-X} + (%S−$X^{\ddagger}$)D_{S-X}.

TABLE 1: Predicted Bond Lengths (Å), Vibrational Frequencies (cm^{-1}), Dipole Moments (D), and Dissociation Energies (kJ/mol) of LiX (X = Cl, Br, I)

species	level	r(X−Li)	ν	μ	D_{Li-X}
LiCl	G2M(+)	2.024 (2.056)[a]	640	7.080	470.4
	exptl[b]	2.021	643	7.085	469.0 (±13)[c]
LiBr	G2M(+)-ECP	2.191	555	7.210	408.6
	exptl	2.170	563	7.226	418.8 (±4.2)
LiI	G2M(+)-ECP	2.397	496	7.338	344.4
	exptl	2.392	498	7.428	345.2 (±4.2)

[a] From ref 15b, at MP2(full)/6-31+G(d)level. [b] From ref 26. [c] At 298 K, from ref 27, pp 9-105−9-107.

TABLE 2: Main Geometries for CH_3SX and Dissociation Energies (kJ/mol) for the S−X Bonds (X = Cl, Br, I)

	r(C−S)	r(S−X)	∠C−S−Cl	D_{S-X}
CH_3SCl	1.817 (1.799)[a]	2.093 (2.048)	100.0 (99.4)	271.8
CH_3SBr	1.821	2.250	100.6	224.4
CH_3SI	1.827	2.438	101.4	187.7

[a] The values in parentheses are the MP2(full)/6-31+G(d) optimized results from ref 28.

TABLE 3: Main Geometries for the Inversion Dipole−Dipole (1a−c) and Retention Dipole−Dipole Complexes (1′a−c), Inversion TSs (2a−c), and Retention TSs (2′a−c)

	r(X−Li)	r(Li−S)	r(S−X)	r(C−S)	∠X−S−X
inversion complexes XLi···S(CH_3)X					
X = Cl (**1a**)	2.066	2.432	2.106	1.822	151.0
X = Br (**1b**)	2.238	2.416	2.271	1.828	151.7
X = I (**1c**)	2.441	2.417	2.458	1.834	144.0
retention complexes CH_3SX···LiX					
X = Cl (**1′a**)	2.069	2.588	2.115	1.820	79.4
X = Br (**1′b**)	2.229	2.474	2.253	1.828	101.5
X = I (**1′c**)	2.436	2.455	2.443	1.834	110.8
inversion TSs [X···CH_3SLi···X]‡					
X = Cl (**2a**)	2.739	2.184	2.446	1.832	144.5
X = Br (**2b**)	2.808	2.210	2.616	1.835	141.1
X = I (**2c**)	2.921	2.239	2.824	1.840	138.6
retention TSs [CH_3S···X_2Li]‡					
X = Cl (**2′a**)	2.154	2.784	3.411	1.790	77.9
X = Br (**2′b**)	2.328	2.954	3.550	1.796	81.1
X = I (**2′c**)	2.539	3.188	3.715	1.803	84.4

TABLE 4: G2M(+) Energetics [ΔH(0 K), kJ/mol] of the Reactions LiX + CH_3SX → $XSCH_3$ + LiX (X = Cl, Br, I; Entries S) for the Two Possible Pathways, Inversion and Retention, and Comparison with Reactions LiX + CH_3X → CH_3X + LiX[a]

		ΔH_{comp}		$\Delta H^{‡}_{cent}$		$\Delta H^{‡}_{ovr}$	
X	pathway	S	C	S	C	S	C
Cl	inversion	56.0	56.4	90.6	203.6	34.6	146.9
	retention	61.2		178.3	207.7	117.0	151.3
Br	inversion	57.9	55.8	69.7	174.7	11.8	119.0
	retention	61.9		172.3	199.6	110.4	143.8
I	inversion	59.2	53.4	53.3	150.7	−6.0	97.3
	retention	63.9		174.1	195.8	110.2	142.4

[a] Entries C are from ref 36.

TABLE 5: NPA Charge Distributions of the Inversion TSs (2a−c) in the Reactions LiX + CH_3SX → $XSCH_3$ + LiX (X = Cl, Br, I) at the MP2/6-311+G(3df,2p)//B3LYP/6-311+G(d,p) Level

	[X···CH_3SLi ···X]‡				
X	CH_3	S	Li	X	CH_3SLi
Cl (**2a**)	−0.015	0.294	0.939	−0.609	1.218
Br (**2b**)	−0.015	0.194	0.918	−0.549	1.098
I (**2c**)	−0.019	0.017	0.861	−0.430	0.859

3.4. Overall Barriers and the Factors That Might Influence Their Heights. The overall barrier($\Delta H^{‡}_{ovr}$) is decisive for the rate of chemical reactions in the gas phase, particularly if they occur under low-pressure conditions in which the reaction system is (in good approximation) thermally isolated.[29] As shown in Table 4, the $\Delta H^{‡}_{ovr}$(inv) values for the LiX + CH_3-SX reactions are positive for X = Cl and Br and negative for X = I, decreasing in the order 34.6 kJ/mol (X = Cl) > 11.8 kJ/mol (X = Br) > −6.0 kJ/mol (X = I), implying that the reaction of LiI + CH_3SI is more facile than the other two. The overall barrier differences between the two pathways [$\Delta H^{‡}_{ovr}$-(ret) − $\Delta H^{‡}_{ovr}$(inv)] increase in the order X = Cl (82.4 kJ/mol) < X = Br (98.6 kJ/mol) < X = I (116.2 kJ/mol), suggesting that the inversion pathway is much more favorable for the present systems (eqs 7−9).

Now, we discuss some factors that might influence the overall barrier heights of the inversion pathway. NPA analysis for the inversion TSs (**2a−c**, Table 5) shows a substantial positive charge on the CH_3SLi moiety and can be readily modeled as triple ion valence bond configuration $[X^{-}\cdots(CH_3SLi)^{+}\cdots X^{-}]^{‡}$,

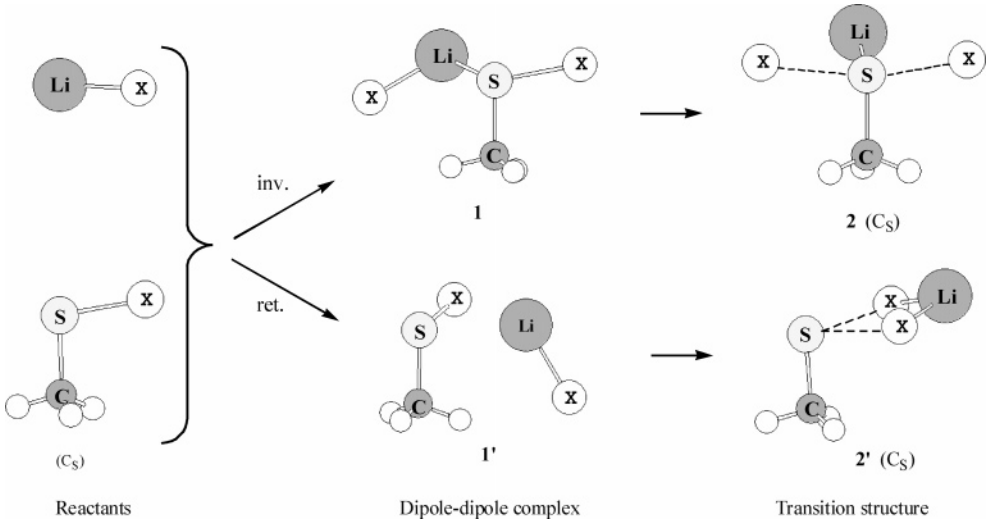

Figure 1. B3LYP/6-311+G(d,p) optimized structures of the reactants, dipole−dipole complexes, and TSs in the ion pair S_N2(S) reactions LiX + $CH_3SX \rightarrow XSCH_3$ + LiX (eqs 7−9). The geometric parameters for all species are listed in Tables 1−3.

although there is no doubt that the covalency plays a significant role in bonding to the entering and leaving groups in the ion pair S_N2(S) TSs. This implies that the contribution of electrostatic interaction may be one of the factors for stabilizing the inversion TSs. Meanwhile, the Li−X bonds in **2a**−**c** are significantly elongated, and the looseness parameters $\%Li-X^{\ddagger}$ decrease in the order X = Cl (32.6) > X = Br (25.5) > X = I (19.7). The data in Tables 1 and 4 indicate that the role of Li−X bond dissociation energies seems to override the electronic interactions and may play a dominant role in determining the overall barrier heights, leading to the highest $\Delta H^{\ddagger}_{ovr}$(inv) for inversion TS LiCl/CH_3SCl (**2a**) because of the strongest Li−Cl bond and the largest $\%Li-Cl^{\ddagger}$ value. The weakest Li−I bond and the smallest $\%Li-I^{\ddagger}$ value may be responsible for the lowest overall barrier for the inversion LiI/CH_3SI TS.

3.5. Possible Origin of the S_N2 Mechanism in the Ion Pair Substitution at Sulfur. As pointed out above, the ion pair nucleophilic substitution at sulfur follows an S_N2 mechanism, in contrast to the A−E mechanism occurring in the corresponding anionic substitution reactions. In this section we will try to analyze the origin of the S_N2 mechanism involved in the ion pair substitution reaction at sulfur from the steric and electronic factors by comparing the geometries and relative energies of the saddle points on the PESs, and address how the stable intermediate in the anionic reaction becomes the transition state in the ion pair reaction. We will take the reactions of $Li^+ + Cl^- + CH_3SCl$ (eq 12) and LiCl + CH_3SCl (eq 7) as examples

$$Li^+ + Cl^- + CH_3SCl \rightarrow CH_3SCl + Cl^- + Li^+ \quad (12)$$

and put the two PESs in Scheme 2, in which the upper and lower PESs represent the anionic and ion pair reactions, respectively, and Li cation is just a spectator to be added in the two sides of the anionic reaction (eq 2) to keep the same stoichiometry for the comparison of total energies. The optimized geometries of species involved in the anionic reaction are presented in Figure 2.

The energies of all the species in Scheme 2 are relative to the free reactants (LiCl + CH_3SCl) in eq 7. It is worth noticing that the energy of incoming TS $[Cl^-\cdots CH_3SCl]^{\ddagger}$ (**4a**) relative to the incoming ion−dipole complex $Cl^-\cdots CH_3SCl$ (**3a**) is ΔH(0 K) = −1.1 kJ/mol and ΔG(298 K) = 3.8 kJ/mol in eq 12, so the relative energies for all species in Scheme 2 are represented by ΔG(298 K). In this way, the PES for eq 12 is a classical

SCHEME 2: Schematic Potential Energy Surface for the Anionic Substitution Reaction $Li^+ + Cl^- + CH_3SCl \rightarrow ClSCH_3 + Cl^- + Li^+$ (upper) and Ion Pair Substitution Reaction LiCl + $CH_3SCl \rightarrow ClSCH_3$ + LiCl (lower)[a]

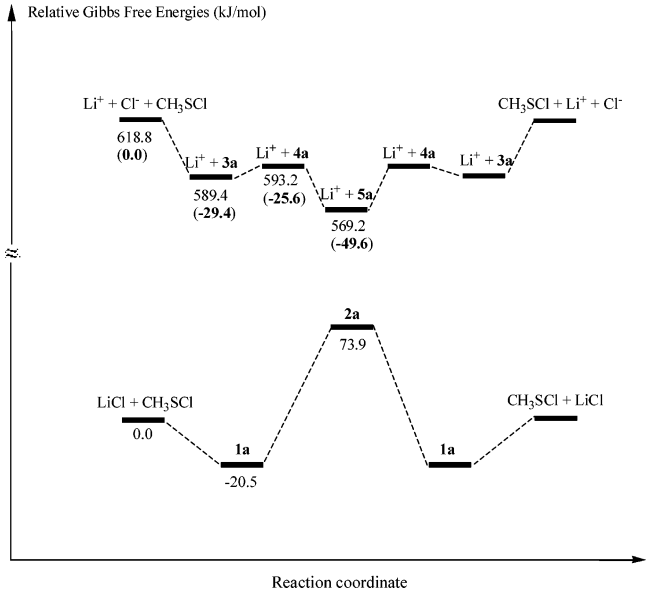

[a] All of the numbers in roman type represent ΔG(298 K) values relative to free reactants (LiCl + CH_3SCl) and the boldface numbers in parentheses are the ΔG(298 K) values relative to $Li^+ + Cl^- + CH_3SCl$.

triple-well curve, indicating that the anionic substitution reaction at the methylsulfenyl sulfur atom follows an A−E mechanism. It is found from Scheme 2 that the relative Gibbs free energy for the free reactants ($Li^+ + Cl^- + CH_3SCl$) is 618.8 kJ/mol, which is actually the heterolytic cleavage energy for the Li−Cl bond in terms of ΔG(298 K).

The combination of Li^+ with Cl^- in **3a** and **4a** will make them collapse to become the inversion dipole−dipole complex $ClLi\cdots S(CH_3)Cl$ (**1a**), whereas the lithium cation binding simultaneously with sulfur and two chlorine atoms in the stable intermediate $[Cl\cdots CH_3S\cdots Cl]^-$ (**5a**) will lead to the inversion TS LiCl/CH_3SCl (**2a**) due to the significant decrease of the Cl−S−Cl bond angle from 177.9° in **5a** to 144.5° in **2a**. In view of the electronic effect, the chloride anion with a localized charge in **3a** and **4a** will be more stabilized by Li cation than the stable

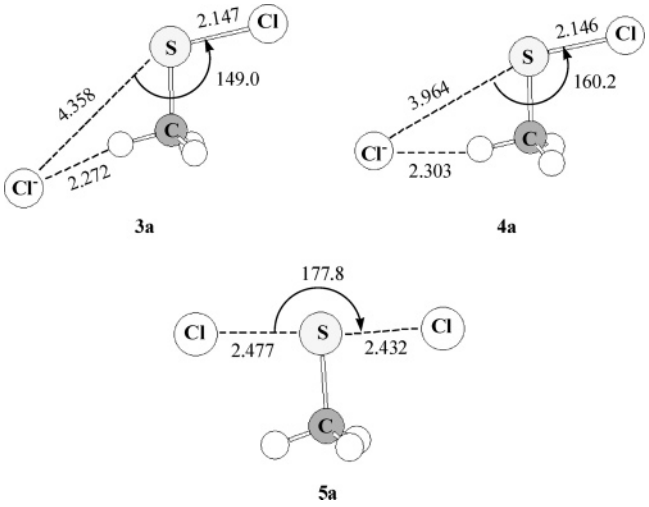

Figure 2. B3LYP/6-311+G(d,p) optimized geometries of the ion−dipole complex, incoming TS, and stable intermediate in the reaction $Cl^- + CH_3SCl \rightarrow ClSCH_3 + Cl^-$.

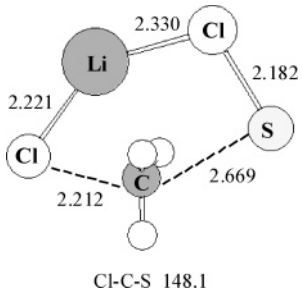

Figure 3. Optimized TS geometry in the ion pair $S_N2(C)$ reaction $LiCl + CH_3SCl \rightarrow ClCH_3 + LiClS$ at the level of B3LYP/6-311+G (d,p).

intermediate (**5a**) bearing more dispersed charge, thus transferring the stable intermediate in the anionic reaction into a transition state in the ion pair reaction. Therefore, some simple interaction from Li^+ can result in a qualitative modification of the PES from anionic to ion pair reaction.

3.6. Ion Pair S_N2 at Carbon: Potential Competition Reaction. When the nucleophile LiX reacts with CH_3SX, ion pair $S_N2(C)$ reaction is another possible reaction channel, in which nucleophile attacks carbon instead of sulfur atom on the substrate CH_3SX, implying that the ion pair $S_N2(C)$ reactions can compete potentially with $S_N2(S)$. In this section, we will compare the possible competition reaction channel from the viewpoints of kinetics and thermodynamics using the reaction of LiCl with CH_3SCl. Our studies show that the reaction enthalpy for the ion pair $S_N2(C)$ reaction (eq 13) is highly

$$LiCl + CH_3SCl \rightarrow ClCH_3 + LiClS \qquad (13)$$

endothermic ($\Delta H_{ovr} = 73.2$ kJ/mol). The calculated overall barrier for eq 13 is 155.6 kJ/mol, much higher than that in the corresponding ion pair $S_N2(S)$ reaction (eq 7) by 121.0 kJ/mol. These results indicate that the $S_N2(C)$ reaction is kinetically and thermodynamically unfavorable. This conclusion can be also applied to other halogens. The substantially larger geometric looseness of the C−S bond (%C−S‡ = 46.6) in the ion pair TS (Figure 3) may be responsible for the higher overall barrier for the ion pair $S_N2(C)$ reaction (eq 13). Moreover, the heterolytic cleavage energy for $CH_3SCl \rightarrow CH_3S^+ + Cl^-$ [ΔH_{het}(S−Cl) = 800.8 kJ/mol] is much lower than that for $CH_3SCl \rightarrow CH_3^+ + ClS^-$ [ΔH_{het}(C−S) = 993.0 kJ/mol] at the G2M(+) level, which relates the better leaving ability of Cl^- than that of ClS^-. Therefore, ion pair nucleophilic substitution at sulfur is much more favorable than at carbon and the ion pair $S_N2(C)$ reactions can be ignored in the present work.

4. Conclusions

Application of G2M(+) theory to the symmetric ion pair exchange reactions on the methylsulfenyl sulfur atom (eqs 7−9) in the gas phase leads to the following conclusions:

(1) The energy profiles are described by double-well curves, indicating the gas-phase ion pair substitution reactions at sulfur proceed along an classic S_N2 pathway. There are two possible reaction channels via different dipole−dipole complexes and different transition structures. Predicted reaction pathways are

inversion:

$$LiX + CH_3SX \rightarrow XLi\cdots S(CH_3)X\ (\mathbf{1a}-\mathbf{c}) \rightarrow [X\cdots CH_3SLi\cdots X]^‡\ (\mathbf{2a}-\mathbf{c}) \rightarrow X(CH_3)S\cdots LiX\ (\mathbf{1a}-\mathbf{c}) \rightarrow CH_3SX + LiX \qquad (X = Cl, Br, \text{and } I)$$

retention:

$$LiX + CH_3SX \rightarrow CH_3SX\cdots LiX\ (\mathbf{1'a}-\mathbf{c}) \rightarrow [CH_3S\cdots X_2Li]^‡\ (\mathbf{2'a}-\mathbf{c}) \rightarrow XLi\cdots XSCH_3\ (\mathbf{1'a}-\mathbf{c}) \rightarrow CH_3SX + LiX \qquad (X = Cl, Br, \text{and } I)$$

(2) The large energy gaps between two possible pathways [$\Delta H^‡_{ovr}$(ret) − $\Delta H^‡_{ovr}$(inv) = 82.4 kJ/mol (X = Cl), 98.6 kJ/mol (X = Br), and 116.2 kJ/mol (X = I)] imply that the inversion pathway is much more favorable for all halogens.

(3) The G2M(+) central barriers for the inversion TSs [X···$CH_3SLi\cdots X]^‡$ increase in the order 90.6 kJ/mol (X = Cl) > 69.7 kJ/mol (X = Br) > 53.3 kJ/mol (X = I) and are found to correlate well with the geometric looseness of the transition state %Li−X‡ + %S−X‡ and bond dissociation energies D_{Li-X} and D_{S-X}.

(4) Even though the ion pair $S_N2(C)$ reaction (eq 13) potentially competes with the ion pair S_N2 (S) reaction (eq 7), calculated results show that the former one is much less favorable from the viewpoints of kinetics and thermodynamics.

Acknowledgment. The authors from Sichuan University are thankful for the financial support from the Scientific Research Foundation for the Returned Chinese Scholars. Y.R. and S.-Y.C. are very thankful to the National Science Council and the Ministry of Education (Contract No. 95-2113-M-007-034-MY2) of Taiwan for their financial support. We express our gratitude to the referees for their valuable comments.

References and Notes

(1) (a) Ren, Y.; Chu, S. Y. *J. Theor. Comput. Chem.* **2006**, *1*, 121. (b) Williams, A. *Concerted Organic and Bio-Organic Mechanisms*; CRC Press: Boca Raton, FL, 2000; Chapter 6, p 159.

(2) (a) Shaik, S. S.; Schlegel, H. B.; Wolfe, S. *Theoretical Aspects of Physical Organic Chemistry, The S_N2 Mechanism*; Wiley: New York, 1992. (b) Laerdahl, J. K.; Uggerud, E. *Int. J. Mass Spectrom.* **2002**, *214*, 277.

(3) (a) Bühl, M.; Schaefer, H. F., III. *J. Am. Chem. Soc.* **1993**, *115*, 9143. (b) Glukhovtsev, M. N.; Pross, A.; Radom, L. *J. Am. Chem. Soc.* **1995**, *117*, 9012. (c) Ren, Y.; Basch, H.; Hoz, S. *J. Org. Chem.* **2002**, *67*, 5891. (d) Ren, Y.; Wolk, J. L.; Hoz, S. *Int. J. Mass Spectrom.* **2002**, *221*, 59. (e) Ren, Y.; Zhu, H. J. *J. Am. Soc. Mass Spectrom.* **2004**, *15*, 673.

(4) (a) Bachrach, S. M. *J. Org. Chem.* **1990**, *55*, 1016. (b) Ren, Y.; Wolk, J. L.; Hoz, S. *Int. J. Mass Spectrom.* **2002**, *220*, 1. (c) Ren, Y.; Wolk, J. L.; Hoz, S. *Int. J. Mass Spectrom.* **2003**, *225*, 167.

(5) (a) Damrauer, R.; DePuy, C. H.; Bierbaum, V. M. *Organometallics* **1982**, *1*, 1553. (b) Davis, L. P.; Burggraf, L. W.; Gordon, M. S.; Baldridge, K. K. *J. Am. Chem. Soc.* **1985**, *107*, 4415. (c) Deiters, J. A.; Holmes, R. R. *J. Am. Chem. Soc.* **1987**, *109*, 1686.

(6) (a) Bachrach, S. M.; Mulhearn, D. C. *J. Phys. Chem.* **1993**, *97*, 12229. (b) Søling, T. I.; Pross, A.; Radom, L. *Int. J. Mass Spectrom.* **2001**, *210/211*, 1.

(7) (a) Ciuffarin, E.; Griselli, F. *J. Am. Chem. Soc.* **1970**, *92*, 6015. (b) Ciuffarin, E.; Guaraldi, G. *J. Org. Chem.* **1970**, *35*, 2006.

(8) Senatore, L.; Ciuffarin, E.; Sagramora, L. *J. Chem. Soc., B* **1971**, *11*, 2191.

(9) (a) Kice, J. L.; Large, G. B. *J. Am. Chem. Soc.* **1968**, *90*, 4069. (b) Kice, J. L.; Rogers, T. E.; Warheit, A. C. *J. Am. Chem. Soc.* **1974**, *96*, 8020. (c) Kice, J. L.; Rogers, T. E. *J. Org. Chem.* **1976**, *41*, 225.

(10) Kice, J. L.; Liu, C. C. A. *J. Org. Chem.* **1979**, *44*, 1918.

(11) Bachrach, S. M.; Mulhearn, D. C. *J. Phys. Chem.* **1996**, *100*, 3535. (b) Mulhearn, D. C.; Bachrach, S. M. *J. Am. Chem. Soc.* **1996**, *118*, 9415. (c) Bachrach, S. M.; Gailbreath, B. D. *J. Org. Chem.* **2001**, *66*, 2005. (d) Bachrach, S. M.; Woody, J. T.; Mulhear, D. C. *J. Org. Chem.* **2002**, *67*, 8983. (e) Bachrach, S. M.; Chamberlin, A. C. *J. Org. Chem.* **2003**, *68*, 4743. (f) Hayes, J. M.; Bachrach, S. M. *J. Phys. Chem. A* **2003**, *107*, 7952. (g) Norton, S. H.; Bachrach, S. M.; Hayes, J. M. *J. Org. Chem.* **2005**, *70*, 5896.

(12) Gai, J. G.; Ren, Y. *Chin. J. Org. Chem.* **2004**, *24*, 1267.

(13) (a) Winstein, S.; Savedoff, L. G.; Smith, S. G.; Stevens, I. D. R.; Gall, J. S. *Tetrahedron Lett.* **1960**, *1* (30), 24. (b) Streitwieser, A.; Juaristi, E.; Kim, Y.-J.; Pugh, J. *Org. Lett.* **2000**, *2*, 3739. (c) Streitwieser, A. *J. Mol. Model.* **2006**, *12*, 673, and references cited therein.

(14) Lai, Z.-G.; Westaway, K. C. *Can. J. Chem.* **1989**, *67*, 21.

(15) (a) Harder, S.; Streitwieser, A.; Petty, J. T.; Schleyer, P. v. R. *J. Am. Chem. Soc.* **1995**, *117*, 3253. (b) Streitwieser, A.; Choy, G. S. C.; Abu-Hasanayn, F. *J. Am. Chem. Soc.* **1997**, *119*, 5013. (c) Leung, S. S. W.; Streitwieser, A. *J. Comput. Chem.* **1998**, *19*, 1325.

(16) (a) Ren, Y.; Chu, S. Y. *J. Comput. Chem.* **2004**, *25*, 461. (b) Ren, Y.; Li, M.; Wong, N. B; Chu, S. Y. *J. Mol. Model.* **2006**, *12*, 182. (c) Sun, Y. X.; Ren, Y.; Wong, N. B.; Chu, S. Y.; Xue, Y. *Int. J. Quantum Chem.* **2006**, *106*, 1653.

(17) (a) Ren, Y.; Chu, S. Y. *Chem. Phys. Lett.* **2003**, *376*, 524. (b) Ren, Y.; Chu, S. Y. *J. Phys. Chem. A* **2004**, *108*, 7079.

(18) Cremlyn, R. J. *An Introduction of Orgranosulfur Chemistry*; John Wiley & Sons: Chichester, U.K., 1996; pp 57 and 95.

(19) Mebel, A. M.; Morokuma, K.; Lin, M. C. *J. Chem. Phys.* **1995**, *103*, 7414.

(20) (a) Zhu, R. S.; Xu, Z. F.; Lin, M. C. *J. Chem. Phys.* **2002**, *116*, 7452. (b) Bui, B. H.; Zhu, R. S.; Lin, M. C. *J. Chem. Phys.* **2002**, *117*, 11188. (c) Tokmakov, I. V.; Park, J.; Gheyas, S.; Lin, M. C. *J. Phys. Chem. A* **1999**, *103*, 3636.

(21) Parthiban, S.; de Oliveira, G.; Martin, J.-M. L. *J. Phys. Chem. A* **2001**, *105*, 895.

(22) (a) Lee, C.; Yang, W.; Parr, R. G. *Phys. Rev. B* **1988**, *37*, 785. (b) Becke, A. D. *J. Chem. Phys.* **1993**, *98*, 5648. (c) Becke, A. D. *J. Chem. Phys.* **1992**, *96*, 2155.

(23) Wadt, W. R.; Hay, P. J. *J. Chem. Phys.* **1985**, *82*, 284.

(24) (a) Reed, A. E.; Weinstock, R. B.; Weinhold, F. *J. Chem. Phys.* **1985**, *83*, 735. (b) Foster, J. P.; Weinhold, F. *J. Am. Chem. Soc.* **1980**, *102*, 7211. (c) Reed, A. E.; Weinhold, F. *J. Chem. Phys.* **1983**, *78*, 4066. (d) Reed, A. E.; Curtiss, L. A.; Weinhold, F. *Chem. Rev.* **1988**, *88*, 899.

(25) Frisch, M. J.; Trucks, G. W.; Schlegel, H. B.; Scuseria, G. E.; Robb, M. A.; Cheeseman, J. R.; Zakrzewski, V. G.; Montgomery, J. A.; Stratmann, R. E., Jr.; Burant, J. C.; Dapprich, S.; Millam, J. M.; Daniels, A. D.; Kudin, K. N.; Strain, M. C.; Farkas, O.; Tomasi, J.; Barone, V.; Cossi, M.; Cammi, R.; Mennucci, B.; Pomelli, C.; Adamo, C.; Clifford, S.; Ochterski, J.; Petersson, G. A.; Ayala, P. Y.; Cui, Q.; Morokuma, K.; Malick, D. K.; Rabuck, A. D.; Raghavachari, K.; Foresman, J. B.; Cioslowski, J.; Ortiz, J. V.; Baboul, A. G.; Stefanov, B. B.; Liu, G.; Liashenko, A.; Piskorz, P.; Komaromi, I.; Gomperts, R.; Martin, R. L.; Fox, D. J.; Keith, T.; Al-Laham, M. A.; Peng, C. Y.; Nanayakkara, A.; Gonzalez, C.; Challacombe, M.; Gill, P.-M. W.; Johnson, B.; Chen, W.; Wong, M. W.; Andres, J. L.; Gonzalez, C.; Head-Gordon, M.; Replogle, E. S.; Pople, J. A. *Gaussian 98*, revision A.9; Gaussian, Inc.: Pittsburgh, PA, 1998.

(26) *NIST Standard Reference Database Number 69*; National Institute of Standards and Technology: Gaithersburg, MD, July 2005.

(27) Lide, D. R. *CRC Handbook of Chemistry and Physics*, 72th ed.; CRC Press: Boca Raton, FL, 1991−1992.

(28) Cheng, B.-M.; Chew, E.-P.; Liu, C.-P.; Yu, J. S. K.; Yu, C. H. *J. Chem. Phys.* **1999**, *110*, 4757.

(29) (a) Nibbering, N. M. M. *Acc. Chem. Res.* **1990**, *23*, 279. (b) Nibbering, N. M. M. *Adv. Phys. Org. Chem.* **1988**, *24*, 1.